The minor sulfur isotope composition of Cretaceous and Cenozoic seawater sulfate

A. L Masterson[1], Boswell A. Wing[2], Adina Paytan[3], James Farquhar[4], and David T Johnston[1]

Corresponding author: D. T. Johnston, Department of Earth and Planetary Sciences, Harvard University, Cambridge MA. (johnston@eps.harvard.edu)

[1]Department of Earth and Planetary Sciences, Harvard University, Cambridge MA.

[2]Department of Geoscience, McGill University, Montreal Canada.

[3]Institute of Marine Sciences, UCSC, Santa Cruz, California.

[4]Department of Geology, University of Maryland, College Park Md.

This article has been accepted for publication and undergone full peer review but has not been through the copyediting, typesetting, pagination and proofreading process, which may lead to differences between this version and the Version of Record. Please cite this article as doi: 10.1002/2016PA002945

The last 125 million years captures major changes in the chemical composition of the ocean and associated geochemical and biogeochemical cycling. The sulfur isotopic composition of seawater sulfate, as proxied in marine barite, is one of the more perplexing geochemical records through this interval. Numerous analytical and geochemical modeling approaches have targeted this record. In this study we extend the empirical isotope record of seawater sulfate to therefore include the two minor sulfur isotopes, ^{33}S and ^{36}S. These data record a distribution of values around means of Δ^{33}S and Δ^{36}S of 0.043 $\pm$ 0.016‰ and -0.39 $\pm$ 0.15‰, which regardless of δ^{34}S-based binning strategy, is consistent with a signal population of values throughout this interval. We demonstrate with simple box modeling that substantial changes in pyrite burial and evaporite sulfate weathering can be accommodated within the range of our observed isotopic values.

Key Points:

- Seawater sulfate barite record exhibits perturbations in ^{34}S and periods of stasis.
- Minor isotope (^{33}S and ^{36}S) demonstrates no statistically significant change throughout 120 Myr.
- Major changes in pyrite burial and sulfate weathering can be accommodated within analytical precision.

1. Introduction

Reconstructing records of seawater sulfate and atmospheric oxygen are central to understanding Earth surface change over the last four billion years [6@Canfield, 2004, 21@Hayes and Waldbauer, 2006]. Through the Phanerozoic, where geological and geochemical records are more robust, more refined estimates of the concentration and isotopic composition of seawater sulfate are possible [1@Bergman et al., 2004, 2@Berner and Canfield, 1989, 29@Kampschulte and Strauss, 2004, 33@Lowenstein et al., 2003, 34@Lowenstein et al., 2001, 39@Paytan et al., 1998, 40@Paytan et al., 2004]. For instance, fluid inclusion records suggest large and bidirectional changes in sulfate concentrations over the Phanerozoic [5@Brennan et al., 2013, 22@Horita et al., 2002, 33@Lowenstein et al., 2003, 34@Lowenstein et al., 2001]. Sulfur isotopic records from various mineral phases are also variable [7@Canfield and Farquhar, 2009, 29@Kampschulte and Strauss, 2004], with the rate of change related to sulfate concentrations [48@Wortmann and Paytan, 2012]. Matching sulfur isotopic and concentration records can, however, be challenging to interpret given the uncertainty associated with any given isotopic or concentration record. Fortunately, a high precision isotopic record is possible for the last 125 Ma - present via authigenic barite minerals extracted from deep sea cores [39@Paytan et al., 1998, 40@Paytan et al., 2004].

The sulfur isotopic composition of seawater sulfate is controlled by the same set of fluxes and mechanisms that establish and drive changes in seawater sulfate concentrations. The controls on both the concentration and isotopic composition of seawater sulfate are sulfate inputs to the ocean via oxidative weathering and evaporite dissolution,

with delivery via rivers [?]. These inputs are countered by sulfur removal through hydrothermal and sedimentary sulfide minerals, as well as sulfate mineral sinks (evaporites, anhydrite, and carbonate associated sulfate). Each of these input and output fluxes carry their own unique, time-dependent isotopic composition [18@Halevy et al., 2012]. The control on each is partly environmental, tectonic, and biological and each carries characteristic timescales for change. At present, however, the large marine sulfate reservoir ($3.9x10^{19}$ mols [41@Petsch and Berner, 1998]) is buffered against perturbations given the long residence time ($\approx 10^7$ years, [8@Claypool et al., 1980]) and resultant well-mixed ocean isotopic composition (e.g. [26@Johnston et al., 2014]). However, this not always the case throughout earlier intervals of earth history when sulfate concentrations may have be substantially lower.

It is within this framework - balancing inputs and outputs - that marine barite records have been interpreted. The composition of seawater sulfate as recorded in barite shows a distinctive and quite perplexing structure (Fig. 1 [30@Kurtz et al., 2003,39@Paytan et al., 1998, 40@Paytan et al., 2004, 48@Wortmann and Paytan, 2012]). Namely, the last 125 Ma is marked by a series of three relatively stable isotopic compositional periods (120-100 Ma, 95-50 Ma, and 45-5Ma), separated by abrupt transitions (denoted by color scheme on figures). Notably, standard approaches thus require either massive and punctuated changes in fluxes or intrinsic fractionations, an exceedingly small sulfate reservoir, or some combination of both. This is simply to satisfy the rate of isotopic change. Further, from first principles, changes in fluxes should manifest as an isotopic decay related to the size of the forcing, and modulated by the residence time of sulfate at that time. In

originally interpreting these records, Paytan and colleagues rightfully evaluated possible biogeochemical and tectonic controls on marine sulfate [39@Paytan et al., 1998]. A more mathematically driven C - S study [30@Kurtz et al., 2003] followed shortly thereafter and, similarly, explored the changes necessary to the sulfur cycle in order to account for barite δ^{34}S records. Often, the interpreted driver of δ^{34}S changes is a major swing in pyrite burial in a low sulfate ocean. Ensuing studies moved away from pyrite burial and brought sulfate evaporite distributions to bear on the δ^{34}S record [48@Wortmann and Paytan, 2012, 47@Wortmann and Chernyavsky, 2007]. For instance, massive evaporite deposition associated with the opening of the south Atlantic in the early Cretaceous [20@Hay et al., 2006, 47@Wortmann and Chernyavsky, 2007, 48@Wortmann and Paytan, 2012] could serve as a large and temporally punctuated sink for sulfate without imposing an extreme isotope effect. The substantial decrease in the standing stock of seawater sulfate, estimated to reach a minimum of $\sim$ 2 mM, thus allows for the rapid ($<$ 5 million years) changes preserved in δ^{34}S between 125 and 50 million years ago. As this hypothesis is framed, much of this gypsum is reintroduced to the ocean at $\sim$ 45 Ma, again an event that would not carry a significant point source of isotopic change in δ^{34}S of sulfate but impose a rapid change to the buffering capacity of the seawater sulfate reservoir.

In this study we present δ^{33}S, δ^{34}S, and δ^{36}S values of marine barite. These analyses are possible only through fluorination to SF_6, and in keeping with minor isotope literature (e.g. [10@Farquhar et al., 2003]), we present these data as Δ^{33}S and Δ^{36}S. The inclusion of minor sulfur isotope data allows for a sensitivity analyses on the mechanisms proposed to explain the published δ^{34}S barite record. Models outlined below explore perturbations to

both pyrite burial and evaporite burial/weathering, each of which would carry a different multiple sulfur isotopic consequence for marine sulfate.

2. Materials and Methods

The barite samples analyzed in this study are the same as those presented previously for the δ^{34}S composition [39@Paytan et al., 1998, 40@Paytan et al., 2004]. For that original work, barite minerals were chemically separated from core material and processed to convert barite to silver sulfide. This Ag_2S was generated prior to our study. Here, we fluorinated Ag_2S to generate SF_6 at both the University of Maryland and Harvard University. In both labs, an excess of F_2 is introduced to a reaction vessel containing the sample. The vessel if heated for $\approx$ 8 hours to ensure a complete conversation of Ag_2S to SF_6. The product SF_6 is cleaned cryogenically and chromatographically prior to introduction to a dual inlet gas source mass spectrometer (Thermo Scientific MAT 253). SF_6 is measured as SF_5^+ at m/e 127, 128, 129 and 131. In both labs, full reproducibility of 1 σ of Δ^{33}S and Δ^{36}S is 0.008‰and 0.2‰, respectively [24@Johnston et al., 2007]. These errors are smaller than that associated with δ^{33}S and δ^{36}S given that the errors are mass-dependently correlated with that of δ^{34}S. We use a standard minor isotope notation to report variance in ^{33}S and ^{36}S. The variability is defined as the deviation from a prediction rooted in low temperature thermodynamic equilibrium. This results in the following two expressions [24@Johnston et al., 2007, 23@Johnston, 2011, 10@Farquhar et al., 2003, 11@Farquhar and Wing, 2003]:

$$\Delta^{33}S = \delta^{33}S - 1000 * ((1 + \delta^{34}S/1000)^{0.515} - 1), \quad (1)$$

$$\Delta^{36}S = \delta^{36}S - 1000 * ((1 + \delta^{34}S/1000)^{1.9} - 1). \quad (2)$$

For these data, we assume a composition of VCDT relative to IAEA-S-1 of -0.3‰, 0.107‰, and -0.5‰for δ^{34}S, Δ^{33}S and Δ^{36}S.

3. Results

The minor isotope records documented below were generated from the same silver sulfide samples (the product of sulfate reduction chemistry [12@Forrest and Newman, 1977]) as reported on previously [39@Paytan et al., 1998,40@Paytan et al., 2004]. This redundancy is used as a test of the higher precision methods. That is, the new δ^{34}S data record is tightly correlated (m = 1.000 ± 0.023; b = 0.015 ± 0.45‰) with published values [39@Paytan et al., 1998,40@Paytan et al., 2004]. Here we add to the δ^{34}S compositions the Δ^{33}S and Δ^{36}S values (Figure 1b, c). The mass-dependent nature of these records leaves the composition and variability of Δ^{33}S smaller than Δ^{36}S offset by a scaling factor that varies around 6.85 [38@Ono et al., 2006], depending on the particular mass law [51@Young et al., 2002,36@Miller, 2002]. Contamination in ^{36}S is common, and as such, anomalously enriched Δ^{36}S values were vetted at the time of analysis. Viewed as an entire time series, the Δ^{33}S varies around a mean of 0.043‰(±0.016‰, 1σ) with no statistically significant trend through time (p = 0.3653; Figure 2). A similar result is captured in Δ^{36}S, where the mean is -0.37‰(±0.14, 1σ) and p = 0.4717 for the 125 Ma record (Figure 2). Notably the composition of the modern ocean is Δ^{33}S = 0.047‰and Δ^{36}S = -0.50‰and is noted as a black circle (with error) in Figures 1 and 2.

4. Discussion

The isotopic variability preserved within marine sulfate records over the last 125 million years can be explained by a combination of purely mass-dependent isotope effects, meaning that the isotopic fractionation mechanisms scale with the mass differences of the isotopes [51@Young et al., 2002, 36@Miller, 2002], and mass conservation effects that arise from the mixing and unmixing of pools with different isotopic compositions (e.g. [9@Farquhar et al., 2007]). This mass-dependence results in a δ^{33}S value that scales to δ^{34}S value offset by a factor that varies from 0.507 to 0.515, whereas the δ^{34}S value versus δ^{36}S value ratio fluctuates around 1.9 [11@Farquhar and Wing, 2003, 23@Johnston, 2011]. This covariance is defined as $^{3x}\lambda$, which approximates the slope of a line on a δ^{33}S versus δ^{34}S plot, or $\ln(^{3x}\alpha)/\ln(^{34}\alpha)$. The same expression can be cast for ^{36}S. Much of the variability within minor sulfur isotope records can be linked to biological activity and metabolic processes that induce fractionations with variable λ because of mixing and unmixing at the cellular level [25@Johnston et al., 2005a, 24@Johnston et al., 2007, 9@Farquhar et al., 2007, 10@Farquhar et al., 2003]. In many cases, these $^{3x}\lambda$ values manifest as resolvable Δ^{3x}S values, providing a potential fingerprint of the processes that influenced a given measured composition (note that the magnitude of change in Δ will vary as a function of the absolute change in δ^{3x}S). Put differently, the specific ^{33}S - ^{34}S - ^{36}S of seawater sulfate should reflect the amalgamation of the biological cycling within the S cycle over the mixing time of that reservoir. This approach holds true in interpreting modern marine sulfate [43@Tostevin et al., 2014, 26@Johnston et al., 2014, 37@Ono et al., 2012, 32@Li et al., 2010], as it does in assessing paleo-environmental records [27@Johnston et al.,

2005b, 49@Wu et al., 2014, 50@Wu et al., 2010, 42@Sim et al., 2015]. Given the larger signal/noise in $\Delta^{33}S$ records when compared to $\Delta^{36}S$ (a result of larger $\Delta^{36}S$ analytical error), mass-dependent studies generally focus on $\Delta^{33}S$. Thus, although we include ^{36}S where necessary, much of the discussion and interpretation only considers ^{33}S systematics. Where this is done, it can be assumed that the inclusion of ^{36}S would result in the same conclusions.

The largest isotopic effects measured within the sulfur cycle are microbial in origin. The two processes capable of generating large $\delta^{34}S$ effects - dissimilatory sulfate reduction and sulfur disproportionation - produce highly resolvable $^{33}\lambda$ [25@Johnston et al., 2005a, 23@Johnston, 2011]. In the case of sulfate reduction, which is responsible for a majority of organic carbon remineralization in marine sediments [28@Jorgensen, 1982], isotopic fractionation scales inversely as a function of metabolic rate [31@Leavitt et al., 2013] and results in $^{33}\lambda$ values less than that predicted for thermodynamic equilibrium (0.5145) [24@Johnston et al., 2007, 10@Farquhar et al., 2003]. At high rates, the $\delta^{34}S$ is small (often approaching 17‰ [16@Goldhaber and Kaplan, 1975, 31@Leavitt et al., 2013]) with a $^{33}\lambda$ near 0.510. At low metabolic rates, much larger $\delta^{34}S$ and $^{33}\lambda$ are observed, often approaching thermodynamic equilibrium values of 70‰and 0.515 for $\delta^{34}S$ and $^{33}\lambda$, respectively [11@Farquhar and Wing, 2003, 24@Johnston et al., 2007, 46@Wing and Halevy, 2014]. Much less is known about disproportionation, however existing data point to a wide range of possible $^{34}S/^{32}S$ fractionation effects, often scaling with both substrate [17@Habicht et al., 1998] and metal availability [3@Bottcher and Thamdrup, 2001]; here, metals serve to scavenge biogenic sulfide, keeping [HS^-] low and helping overall

metabolic energetics. The net effect of disproportionation can, however, be summarized as variable δ^{34}S with $^{3x}\lambda$ always greater than 0.5145 [25@Johnston et al., 2005a]. Importantly, this allows disproportionation to be resolved from effects associated with sulfate reduction, even where δ^{34}S values are similar [27@Johnston et al., 2005b]. The final microbial process of note is sulfide oxidation, which imparts a small ^{34}S/^{32}S isotope effect [14@Fry et al., 1985, 13@Fry et al., 1986, 52@Zerkle et al., 2009] and an unique range of $^{33}\lambda$ values.

4.1. The fidelity of barite records

Barite harvested from marine sediments is inferred to capture the contemporaneous isotopic composition of seawater sulfate [39@Paytan et al., 1998]. That is, core top barite is statistically indistinguishable from modern water column sulfate. This was recently confirmed through a series of studies on modern seawater sulfate [26@Johnston et al., 2014, 43@Tostevin et al., 2014, 50@Wu et al., 2010, 37@Ono et al., 2012], yielding a composition of δ^{34}S = 21.14± (0.15)‰, Δ^{33}S, = 0.048± (0.006)‰, and Δ^{36}S = -0.5± (0.20)‰. In comparison, modern core top barite reported here measure at 20.81± (0.2)‰, 0.038± (0.008)‰, and -0.45± (0.2)‰in δ^{34}S, Δ^{33}S, and Δ^{36}S - statistically indistinguishable from modern seawater. The correspondence in sulfur isotope composition between seawater sulfate and core top barite is consistent with the suggested long residence time of sulfate and the use of marine barite as a proxy for the isotopic composition of seawater sulfate in the past.

4.2. A 125 million year record of seawater sulfate

The interpretation of barite records can be approached with a number of different goals. First, when the data are coarsely binned according to the time domains displayed in Figure 1 (see also Figure 3), the entire 125 Ma data set is not normally distributed (according to a D'Agostino and Pearson normality test) in ^{33}S or ^{36}S. For ^{33}S, this may provide real insight into the nature of the variance, meaning that the mechanisms operating on the S cycle are more likely to enrich ^{33}S than deplete it, with the mean value reflecting some more robust steady-state condition or compositional 'floor' (i.e. a common state of the sulfur cycle represented by a lower $\Delta^{33}S$ value) . However, the asymmetry in ^{36}S is possibly analytical. As noted above, contamination on the m/e 131 (where ^{36}S is measured as $^{36}SF_5^+$) will pull $\Delta^{36}S$ compositions toward more enriched values, which is the direction of the skew of the data. Of the more data-rich bins (the most recent 3 geological bins, with n = 11, 32 and 27), most of the data is in fact normally distributed for both $\Delta^{33}S$ values and $\Delta^{36}S$ values for a given time domain. This reinforces arguments made on an average composition of those bins. The exceptions are the 49-98 million year bin in $\Delta^{33}S$ values and the 0-10 million year bin in $\Delta^{36}S$ values. This is evident in the box and whisker analysis in Figure 3, where the asymmetry is evident in the 95% confidence intervals.

Despite the nature of the distributions, Figure 2 demonstrates the mass-dependence of the barite record and illustrates that little to no change in $\Delta^{33}S$ values and $\Delta^{36}S$ values accompanies the small (but resolvable) $\delta^{34}S$ record. As noted above, this is perhaps not unexpected, however does limit the available mechanisms that could be underpinning the $\delta^{34}S$ transitions. Recall that the nature of mass-dependent fractionation predicts that

for any given change in δ^{34}S value, an accompanying magnitude of change in Δ^{33}S value and Δ^{36}S value is expected – the absolute change will be a function of both how far $^{33}\lambda$ values varies from the reference values of 0.515 and 1.9 that are used to define the values of Δ^{33}S and Δ^{36}S = 0, and the magnitude of the change in δ^{34}S. The change in mass law will be linked to the process driving the isotope change. For example, the early Eocene transition is marked by a 4‰change in δ^{34}S, but an unresolvable signal in Δ^{33}S and Δ^{36}S. If this event was triggered solely as a result of reasonable changes in the fractionation associated with sulfate reduction (setting all other factors aside for the moment) at a $^{33}\lambda$ of 0.510 and $^{36}\lambda$ 1.95, then the associated changes in Δ^{33}S value and Δ^{36}S value would be roughly 0.02‰and 0.2‰, respectively. As our measurement analytical uncertainty is similar in magnitude to the expected signal, actually 'seeing' this event in ^{33}S and ^{36}S would be near our analytically resolvable limit and thus unlikely. In order for a unique minor isotope effect to be discernible then, the δ^{34}S would have to be larger, or the $^{33}\lambda$ and $^{36}\lambda$ would have to deviate more significantly from the reference line value. Thus, it is perhaps not unexpected that no resolvable minor isotope signal exists associated with the early Eocene change in δ^{34}S. The example presented here could also be viewed as a simple sensitivity analysis of the capacity for the minor sulfur isotopes to capture large, resolvable effect when viewed in light of the δ^{34}S variability captured over the last 125 million years. Note that in a proper statistical analysis of the entire 125 million year time series, values of both Δ^{33}S and Δ^{36}S are unchanged (Figure 1b,c and Figure 2). This places constraints on the type of changes undergone by the sulfur cycle over the last 125

Ma, and places limits on how changes in certain fluxes might be contributing to these records.

This treatment can be handled more rigorously. In traditionally interpreting δ^{34}S records, the fraction of sulfur leaving the oceans as pyrite (f_{py}) is commonly the metric of interest [2@Berner and Canfield, 1989, 6@Canfield, 2004, 7@Canfield and Farquhar, 2009]. In such treatments, the microbial effects are often summarized as single, constant fractionation factor (captured as $^{34}\epsilon$) so that the only variable is the fraction of burial [30@Kurtz et al., 2003, 19@Halverson and Hurtgen, 2007]. In much the same way, there are isotopic consequences in ^{33}S and ^{36}S that relate how mass is partitioned within the marine sulfur cycle. The difference comes from with the varying definitions of various isotope notations. Mixing relationships are effectively linear in δ^{3x}S but non-linear in Δ^{3x}S. This is more thoroughly discussed elsewhere [9@Farquhar et al., 2007, 23@Johnston, 2011].

In order to test the sensitivity of the isotopic composition of sulfate, and specifically Δ^{33}S values, to the fluctuations that must in some fashion relate to the changes preserved in the δ^{34}S record (pyrite burial, etc.) we have constructed a pseudo steady-state box model. Using this simple approach we test the capacity to induce a change in Δ^{33}S values as a function of the companion δ^{34}S values. Recall that these effects are mass-dependent, so the change in both metrics is necessarily coupled. For this analysis, we arbitrarily chose a perturbation in the magnitude of pyrite burial. Following along the lines of similarly published models (e.g. [30@Kurtz et al., 2003, 15@Gill et al., 2007]), weathering rates are held constant, and pyrite burial rates are doubled over the course of 1 million years.

The isotopic compositions (δ^{34}S and Δ^{33}S values) of all fluxes are held constant. For the weathering input, we have used $F_w = 1.5\text{x}10^{12}$ mol S/yr, and a constant flux of evaporite deposition of $F_{ev} = 1.05\text{x}10^{12}$. Pyrite burial was initially held constant at $4.5\text{x}10^{11}$ mol S/yr, and doubled over 1 Myr to $9.0\text{x}10^{11}$ mol S/yr. Fractionation due to pyrite burial was also held constant at $^{34}\epsilon = 35$ ‰($^{34}\alpha = 0.965$), independent of variability within the burial flux. Finally, we have explored two different cases, with the starting concentration of $[SO_4^{2-}]_0 = 5$ mM and $[SO_4^{2-}]_0 = 25$ mM. The concentration of sulfate was allowed to evolve accordingly.

To introduce isotope systematics to the model, we have used isotope ratios directly, and utilized the trace-abundance approximation ($^{32}F \equiv F$) [9@Farquhar et al., 2007]. In this case, the bulk mass-balance equations for a single box ocean can be written as:

$$\frac{dM_0}{dt} = F_w - F_{ev} - F_{py}, \tag{3}$$

where $\frac{dM_0}{dt}$ is this the rate of change in the concentration of the seawater sulfate reservoir, and F_w, F_{ev}, and F_{py} are the weathering, evaporite deposition, and pyrite burial fluxes, respectively. The isotope mass balance equation (e.g. for ^{34}S) can be written accordingly:

$$\frac{d}{dt}[M_{oc} * {}^{34}R_{oc}] = F_w * {}^{34}R_w - F_{ev} * {}^{34}R_{ev} - F_{py} * {}^{34}R_{py}. \tag{4}$$

Expanding equation 4, incorporating equation 3, and assuming that $^{34}R_{ev} = {}^{34}R_{oc}$, yields the following non-steady state equations, in this case written for ^{33}S and ^{34}S:

$$\frac{d^{33}R_{oc}}{dt} = \frac{1}{M_{oc}}\left[F_w[{}^{33}R_w - {}^{33}R_{oc}] - F_{py}[{}^{33}R_{py} - {}^{33}R_{oc}]\right] \tag{5}$$

$$\frac{d^{34}R_{oc}}{dt} = \frac{1}{M_{oc}}\left[F_w[^{34}R_w - {}^{34}R_{oc}] - F_{py}[^{34}R_{py} - {}^{34}R_{oc}]\right] \quad (6)$$

Assuming that the fractionation associated pyrite deposition remains constant, the following substitution can be made:

$$\frac{d^{33}R_{oc}}{dt} = \frac{1}{M_{oc}}\left[F_w[^{33}R_w - {}^{33}R_{oc}] - F_{py} * {}^{33}R_{oc}[^{33}\alpha_{py} - 1]\right] \quad (7)$$

$$\frac{d^{34}R_{oc}}{dt} = \frac{1}{M_{oc}}\left[F_w[^{34}R_w - {}^{34}R_{oc}] - F_{py} * {}^{34}R_{oc}[^{34}\alpha_{py} - 1]\right] \quad (8)$$

Using a finite difference approach, equations 7 and 8 can thus be solved for the case where both M_0 and ${}^{3x}R_0$ are changing with time. Figure 5 demonstrates the model output the cases where $[SO_4^{2-}]_0 = 5$ and 25mM. In both cases, a doubling of the pyrite burial flux for 1 million years (distributed as a Gaussian) produces positive excursion in the $\delta^{34}S$ value of the ocean from the initial value of $\delta^{34}S = 15.2$ ‰. As expected, the rate of increase varies inversely with the initial size of the sulfate reservoir. Notably, a new 'steady-state' value of $\delta^{34}S$ is not reached in the $[SO_4^{2-}]_0 = 25$ mM case, due to the long residence time of sulfate in the ocean.

Introducing ^{33}S systematics, in both cases, a doubling of the pyrite burial flux yields subtle variations in the evolution of $\delta^{34}S_{oc}$. Using ${}^{33}\lambda$ representative of microbial sulfate reduction (e.g. ${}^{33}\lambda = 0.512$-0.514), the evolution of $\Delta^{33}S_{oc}$ positively correlated with the evolution of $\delta^{34}S_{oc}$, but the magnitude of the change from the initial value (set at $\Delta^{33}S_{oc} = 0.047$ ‰), though measurable, is small ($\pm$ 0.01‰). Thus, even with a large perturbation in $\delta^{34}S_{oc}$ associated with a doubling of a pyrite burial flux, the sensitivity of $\Delta^{33}S_{oc}$ to

the same perturbation is small, and would be difficult to detect within the range of $\delta^{34}S_{oc}$ variability within the last 120 Myr (e.g. $\delta^{34}S_{oc}$ = 15-22 ‰).

Along similar lines, it is possible to test the case where a substantial contribution from an evaporitic source (e.g. [48@Wortmann and Paytan, 2012]) produces a perturbation in the isotopic composition of $\delta^{34}S_{oc}$ and $\Delta^{33}S_{oc}$ values. Although this can be incorporated into a steady-state model like the previous pyrite burial case, a mixture between two different isotopic end-member sources can be used to demonstrate the range of isotopic values that would result from the contribution of a large evaporitic source (i.e. a simple mixing calculation). To do so, it is necessary to assume an evaporite composition - we suggest it falls within the range of isotopic values measured for barite within this study ($\delta^{34}S$ = 15-22 ‰and $\Delta^{33}S$ = 0.02-0.08 ‰). The resulting mixture is a linear combination of the two isotopic sources, with f_{ev} is the fractional contribution of evaporitic sulfate to total seawater, and can be calculated as follows:

$$\delta^{33}S_{mix} = \delta^{33}S_{oc}(1 - f_{ev}) + f_{ev}\delta^{33}S_{ev} \quad (9)$$

$$\delta^{34}S_{mix} = \delta^{34}S_{oc}(1 - f_{ev}) + f_{ev}\delta^{34}S_{ev} \quad (10)$$

The $\delta^{34}S$ and $\Delta^{33}S$ values are of course, functions both of the end-member compositions and f_{ev}. Isotope mass-balance would then indicate that $\delta^{34}S$ and $\Delta^{33}S$ values must fall within the range prescribed by the two end-members. For example, mixing between seawater sulfate sharing the composition of modern sulfate ($\delta^{34}S$ = 21.15 ‰and $\Delta^{33}S$ = 0.047‰) and an evaporite source with ($\delta^{34}S$ = 15 ‰and $\Delta^{33}S$ = 0.02 ‰), gives the mixing

relationship seen in Fig 6. Simply, the mixture between seawater sulfate and an evaporitic source sharing isotopically similar Δ^{33}S values falls within the range of Δ^{33}S barite values measured here. Resolving a contribution from an evaporitic source using Δ^{33}S would require values statistically distinct from those inferred to exist from the composition of sulfate, at least through the latter half of the Phanerozoic.

Conclusions

The development of new isotopic systems and proxies is frequently followed by the critical generation of time-series for those metrics. This study serves the role of providing a robust quantification of the minor sulfur isotope records of seawater sulfate of the late Cretaceous and Cenozoic. Pre-existing δ^{34}S records stand as one of the more under-constrained of the major oceanographic chemical records. The new minor sulfur isotope data presented in this study record invariant Δ^{33}S and Δ^{36}S associated with the swings of up to 5 ‰in δ^{34}S. Models built to include the minor S isotopes can accommodate major changes in pyrite burial and sulfate influxes/outfluxes within the range of compositions measured. That being said, during intervals of Earth history with larger δ^{34}S changes in sulfate (i.e. Phanerozoic or Precambrian), Δ^{33}S and Δ^{36}S should be more easily interpretable metrics (e.g. [49@Wu et al., 2014]). In looking forward, perhaps improved minor isotope precisions, along with a closer association with δ^{18}O records [44@Turchyn and Schrag, 2004, 45@Turchyn and Schrag, 2006], global models of sulfur cycling and sulfate reduction [4@Bowles et al., 2014], and diagenetic modeling studies [35@Masterson et al.,] will further constrain the information held within sulfate records.

Acknowledgments

We would like to thank ten years of conference goers for listening about and commenting on these data. We thank NSF EAR/IF (DTJ), NASA Exobiology (DTJ, JF, AM), NAI (DTJ, JF), NSF-OCE (AP), and NSF EAR (DTJ, JF). Erin Beirne, Ben Gill and many others are thanked for productive discussions. All data is included with this submission as an excel file. All questions about data generation and handling are referred to the corresponding author.

References

Bergman, N. M., Lenton, T. M., and Watson, A. J. (2004). Copse: A new model of biogeochemical cycling over phanerozoic time. *American Journal of Science*, 304(5):397.

Berner, R. A. and Canfield, D. E. (1989). A new model for atmospheric oxygen over phanerozoic time. *Am J Sci*, 289(4):333–61.

Bottcher, M. and Thamdrup, B. (2001). Anaerobic sulfide oxidation and stable isotope fractionation associated with bacterial sulfur disproportionation in the presence of mno2. *Geochimica et Cosmochimica Acta*, 65.

Bowles, M. W., Mogollón, J. M., Kasten, S., Zabel, M., and Hinrichs, K.-U. U. (2014). Global rates of marine sulfate reduction and implications for sub-sea-floor metabolic activities. *Science*, 344(6186):889–91.

Brennan, S. T. . T., Lowenstein, T. K. . K., and Cendon, D. I. . I. (2013). The major-ion composition of cenozoic seawater: The past 36 million years from fluid inclusions in marine halite. *American Journal of Science*, 313(8):713–775.

Canfield, D. E. (2004). The evolution of the earth surface sulfur reservoir. *American Journal of Science*, 304(10):839.

Canfield, D. E. and Farquhar, J. (2009). Animal evolution, bioturbation, and the sulfate concentration of the oceans. *Proc Natl Acad Sci U S A*, 106(20):8123–7.

Claypool, G. E., Holser, W. T., Kaplan, I. R., Sakai, H., and Zak, I. (1980). The age curves of sulfur and oxygen isotopes in marine sulfate and their mutual interpretation. *Chemical Geology*, 28:199–260.

Farquhar, J., Johnston, D. T., and Wing, B. A. (2007). Implications of conservation of mass effects on mass-dependent isotope fractionations: Influence of network structure on sulfur isotope phase space of dissimilatory sulfate reduction. *Geochimica et Cosmochimica Acta*, 71(24):5862–5875.

Farquhar, J., Johnston, D. T., Wing, B. A., Habicht, K. S., Canfield, D. E., Airieau, S., and Thiemens, M. H. (2003). Multiple sulphur isotopic interpretations of biosynthetic pathways: implications for biological signatures in the sulphur isotope record. *Geobiology*, 1(1):27–36.

Farquhar, J. and Wing, B. A. (2003). Multiple sulfur isotopes and the evolution of the atmosphere. *Earth and Planetary Science Letters*, 213(1-2):1–13.

Forrest, J. and Newman, L. (1977). Silver 110 microgram sulfate analysis for the short time resolution of ambient levels of sulfur aerosols. *Analytical Chemistry*, 49(11):1579–1584.

Fry, B., Cox, J., Gest, H., and Hayes, J. M. (1986). Discrimination between 34s and 32s during bacterial metabolism of inorganic sulfur compounds. *J Bacteriol*, 165(1):328–

30.

Fry, B., Gest, H., and Hayes, J. M. (1985). Isotope effects associated with the anaerobic oxidation of sulfite and thiosulfate by the photosynthetic bacterium, chromatium vinosum. *FEMS Microbiol Lett*, 27:227–32.

Gill, B. C., Lyons, T. W., and Saltzman, M. R. (2007). Parallel, high-resolution carbon and sulfur isotope records of the evolving paleozoic marine sulfur reservoir. *Palaeogeography, Palaeoclimatology, Palaeoecology*, 256(3-4):156–173.

Goldhaber, M. and Kaplan, I. (1975). Controls and consequences of sulfate reduction rates in recent marine sediments. *Soil Science*, 119(1):42–55.

Habicht, K. S., Canfield, D. E., and Rethmeier, J. (1998). Sulfur isotope fractionation during bacterial reduction and disproportionation of thiosulfate and sulfite. *Geochimica et Cosmochimica Acta*, 62(15):2585–2595.

Halevy, I., Peters, S. E. . E., and Fischer, W. W. . W. (2012). Sulfate burial constraints on the phanerozoic sulfur cycle. *Science*, 337(6092):331–334.

Halverson, G. P. and Hurtgen, M. T. (2007). Ediacaran growth of the marine sulfate reservoir. *Earth and Planetary Science Letters*, 263(1-2):32–44.

Hay, W. W., Migdisov, A., Balukhovsky, A. N., Wold, C. N., Flögel, S., and Söding, E. (2006). Evaporites and the salinity of the ocean during the phanerozoic: Implications for climate, ocean circulation and life. *Palaeogeography, Palaeoclimatology, Palaeoecology*, 240(1-2):3–46.

Hayes, J. M. and Waldbauer, J. R. (2006). The carbon cycle and associated redox processes through time. *Philos Trans R Soc Lond B Biol Sci*, 361(1470):931–50.

Horita, J., Zimmermann, H., and Holland, H. (2002). Chemical evolution of seawater during the phanerozoic: Implications from the record of marine evaporites. *Geochimica et Cosmochimica Acta*, 66.

Johnston, D. T. (2011). Multiple sulfur isotopes and the evolution of earth's surface sulfur cycle. *Earth-Science Reviews*.

Johnston, D. T., Farquhar, J., and Canfield, D. E. (2007). Sulfur isotope insights into microbial sulfate reduction: When microbes meet models. *Geochimica et cosmochimica acta*, 71(16):3929–3947.

Johnston, D. T., Farquhar, J., Wing, B. A., Kaufman, A. J., Canfield, D. E., and Habicht, K. S. (2005a). Multiple sulfur isotope fractionations in biological systems: A case study with sulfate reducers and sulfur disproportionators. *American Journal of Science*, 305(6-8):645.

Johnston, D. T., Gill, B. C., Masterson, A., Beirne, E., Casciotti, K. L., Knapp, A. N., and Berelson, W. (2014). Placing an upper limit on cryptic marine sulphur cycling. *Nature*, 513(7519):530–3.

Johnston, D. T., Wing, B. A., Farquhar, J., Kaufman, A. J., Strauss, H., Lyons, T. W., Kah, L. C., and Canfield, D. E. (2005b). Active microbial sulfur disproportionation in the mesoproterozoic. *Science*, 310(5753):1477–9.

Jorgensen, B. B. (1982). Mineralization of organic matter in the sea bedthe role of sulphate reduction. *Geochimica et Cosmochimica Acta*.

Kampschulte, A. and Strauss, H. (2004). The sulfur isotopic evolution of phanerozoic seawater based on the analysis of structurally substituted sulfate in carbonates.

Chemical Geology, 204(3-4):255–286.

Kurtz, A. C., Kump, L. R., Arthur, M. A., Zachos, J. C., and Paytan, A. (2003). Early cenozoic decoupling of the global carbon and sulfur cycles. *Paleoceanography*, 18(4):n/a–n/a.

Leavitt, W. D., Halevy, I., Bradley, A. S., and Johnston, D. T. (2013). Influence of sulfate reduction rates on the phanerozoic sulfur isotope record. *Proc Natl Acad Sci U S A*, pages 11244–11249.

Li, X., Gilhooly, W. P., Zerkle, A. L., Lyons, T. W., Farquhar, J., Werne, J. P., Varela, R., and Scranton, M. I. (2010). Stable sulfur isotopes in the water column of the cariaco basin. *Geochimica et Cosmochimica Acta*, 74(23):6764–6778.

Lowenstein, T., Hardie, L., Timofeeff, M., and Demicco, R. (2003). Secular variation in seawater chemistry and the origin of calcium chloride basinal brines. *Geology*, 31:857–860.

Lowenstein, T. K., Timofeeff, M. N., Brennan, S. T., Hardie, L. A., and Demicco, R. V. (2001). Oscillations in phanerozoic seawater chemistry: evidence from fluid inclusions. *Science*, 294(5544):1086–8.

Masterson, A., Alperin, M., Berelson, W., and Johnston, D. Multiple sulfur isotopic insight into sulfur cycling within anoxic sediments within the california-mexico margin; alfonso basin. *Geochimica et Cosmochimica Acta*.

Miller, M. (2002). Isotopic fractionation and the quantification of 17o anomalies in the oxygen three isotope system: an appraisal and geochemical significance. *Geochimica et Cosmochimica Acta*, 66:1881–1889.

Ono, S., Keller, N. S., Rouxel, O., and Alt, J. C. (2012). Sulfur-33 constraints on the origin of secondary pyrite in altered oceanic basement. *Geochimica et Cosmochimica Acta*, 87:323–340.

Ono, S., Wing, B., Johnston, D., Farquhar, J., and Rumble, D. (2006). Mass-dependent fractionation of quadruple stable sulfur isotope system as a new tracer of sulfur biogeochemical cycles. *Geochimica et Cosmochimica Acta*, 70(9):2238–2252.

Paytan, A., Kastner, M., Campbell, D., and Thiemens, M. H. (1998). Sulfur isotopic composition of cenozoic seawater sulfate. *Science*, 282(5393):1459–62.

Paytan, A., Kastner, M., Campbell, D., and Thiemens, M. H. (2004). Seawater sulfur isotope fluctuations in the cretaceous. *Science*, 304(5677):1663–5.

Petsch, S. T. and Berner, R. A. (1998). Coupling the geochemical cycles of c, p, fe, and s; the effect on atmospheric o 2 and the isotopic records of carbon and sulfur. *American Journal of Science*, 298(3):246.

Sim, M. S., Ono, S., and Hurtgen, M. T. (2015). Sulfur isotope evidence for low and fluctuating sulfate levels in the late devonian ocean and the potential link with the mass extinction event. *Earth and Planetary Science Letters*, 419:52–62.

Tostevin, R., Turchyn, A., Farquhar, J., Johnston, D., Eldridge, D., Bishop, J., and McIlvin, M. (2014). Multiple sulfur isotope constraints on the modern sulfur cycle. *Earth and Planetary Science Letters*, 396.

Turchyn, A. V. and Schrag, D. P. (2004). Oxygen isotope constraints on the sulfur cycle over the past 10 million years. *Science*, 303(5666):2004–7.

Turchyn, A. V. and Schrag, D. P. (2006). Cenozoic evolution of the sulfur cycle: Insight from oxygen isotopes in marine sulfate. *Earth and Planetary Science Letters*, 241(3-4):763–779.

Wing, B. A. and Halevy, I. (2014). Intracellular metabolite levels shape sulfur isotope fractionation during microbial sulfate respiration. *Proc Natl Acad Sci U S A*, pages 1–10.

Wortmann, U. G. and Chernyavsky, B. M. (2007). Effect of evaporite deposition on early cretaceous carbon and sulphur cycling. *Nature*, 446(7136):654–6.

Wortmann, U. G. . G. and Paytan, A. (2012). Rapid variability of seawater chemistry over the past 130 million years. *Science*, 337(6092):334–336.

Wu, N., Farquhar, J., and Strauss, H. (2014). δ34s and δ33s records of paleozoic seawater sulfate based on the analysis of carbonate associated sulfate. *Earth and Planetary Science Letters*, 399:44–51.

Wu, N., Farquhar, J., Strauss, H., Kim, S. T., and Canfield, D. E. (2010). Evaluating the s-isotope fractionation associated with phanerozoic pyrite burial. *Geochimica et Cosmochimica Acta*, 74(7):2053–2071.

Young, E. D., Galy, A., and Nagahara, H. (2002). Kinetic and equilibrium mass-dependent isotope fractionation laws in nature and their geochemical and cosmochemical significance. *Geochimica et Cosmochimica Acta*, 66(6):1095–1104.

Zerkle, A. L., Farquhar, J., Johnston, D. T., Cox, R. P., and Canfield, D. E. (2009). Fractionation of multiple sulfur isotopes during phototrophic oxidation of sulfide and elemental sulfur by a green sulfur bacterium. *Geochimica et Cosmochimica Acta*,

73(2):291–306.

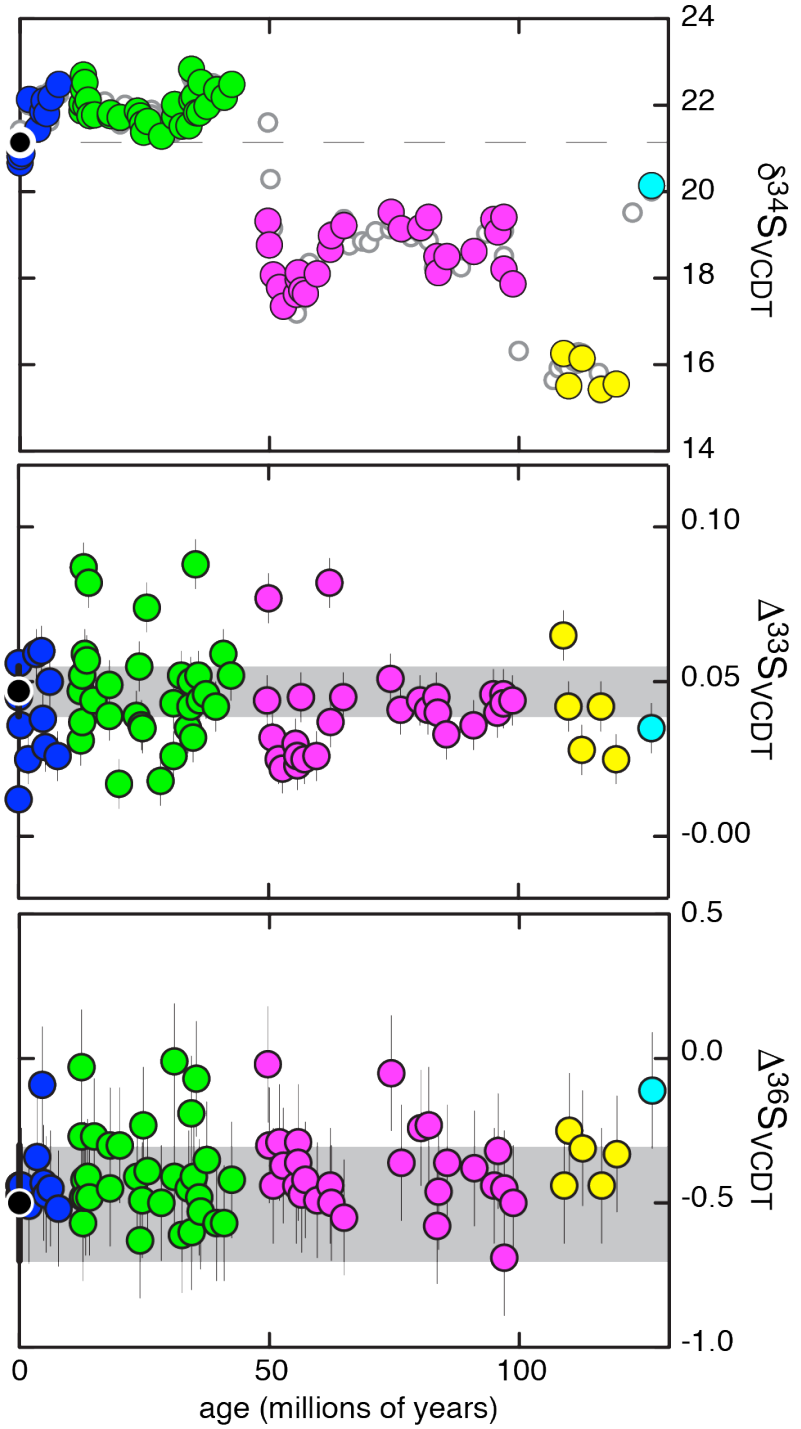

Figure 1. The barite record of δ^{34}S, Δ^{33}S, and Δ^{36}S versus time for the Cretaceous and Cenozoic (frames A-C, respectively). Samples in gray (background in Frame A) are previously published, whereas those in color represent this study. This color code is used throughout and based on δ^{34}S compositions. Errors are 2 σ. All data placed on a common V-CDT scale. Gray bar across each frame is the composition (and error) of the modern marine sulfate reservoir [26@Johnston et al., 2014, 43@Tostevin et al., 2014].

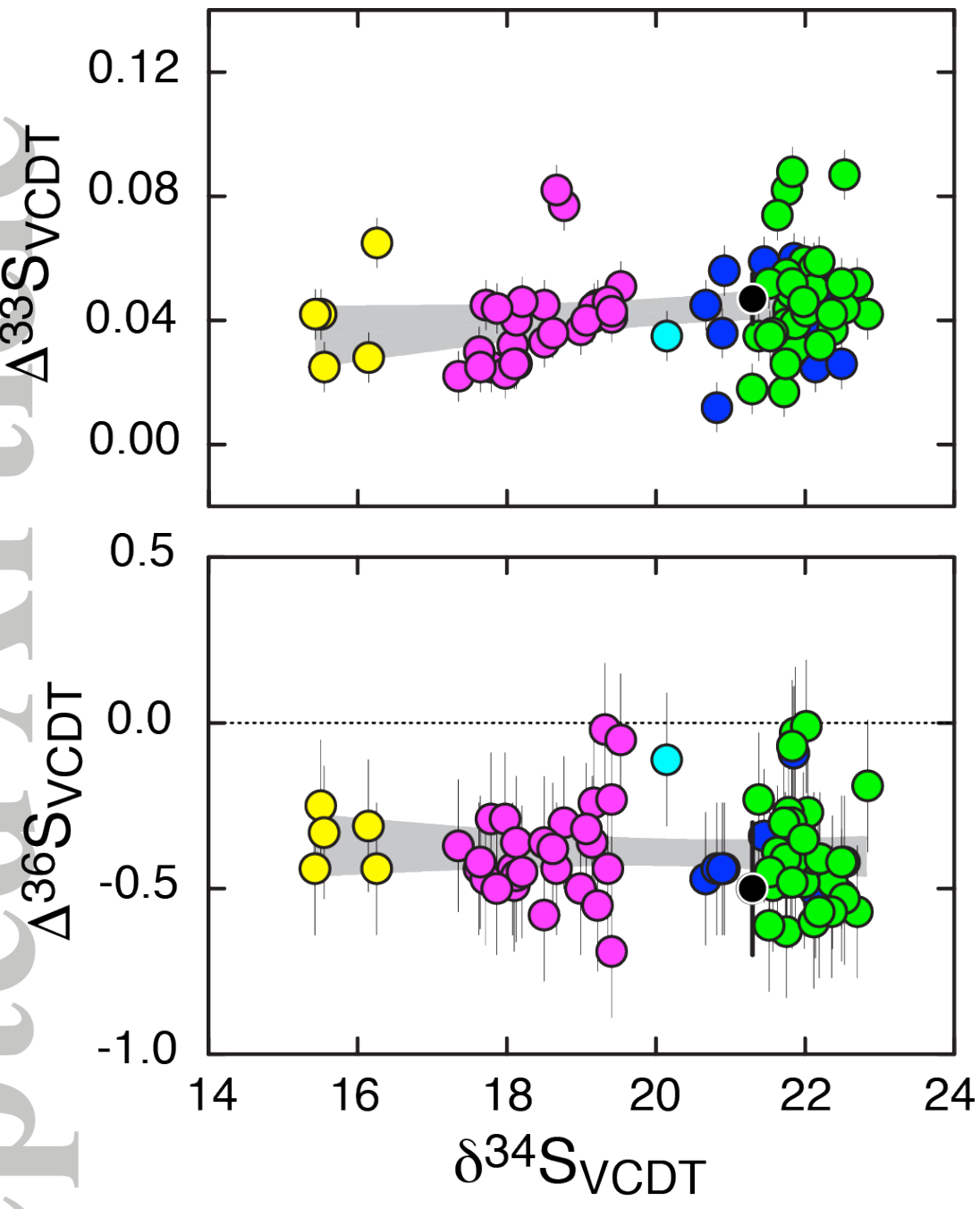

Figure 2. The δ^{34}S versus Δ^{33}S and Δ^{36}S for the samples presented in Figure 1 (same color coding).. Errors are 2 σ. The regression reflect a 95% confidence interval on the entire population.

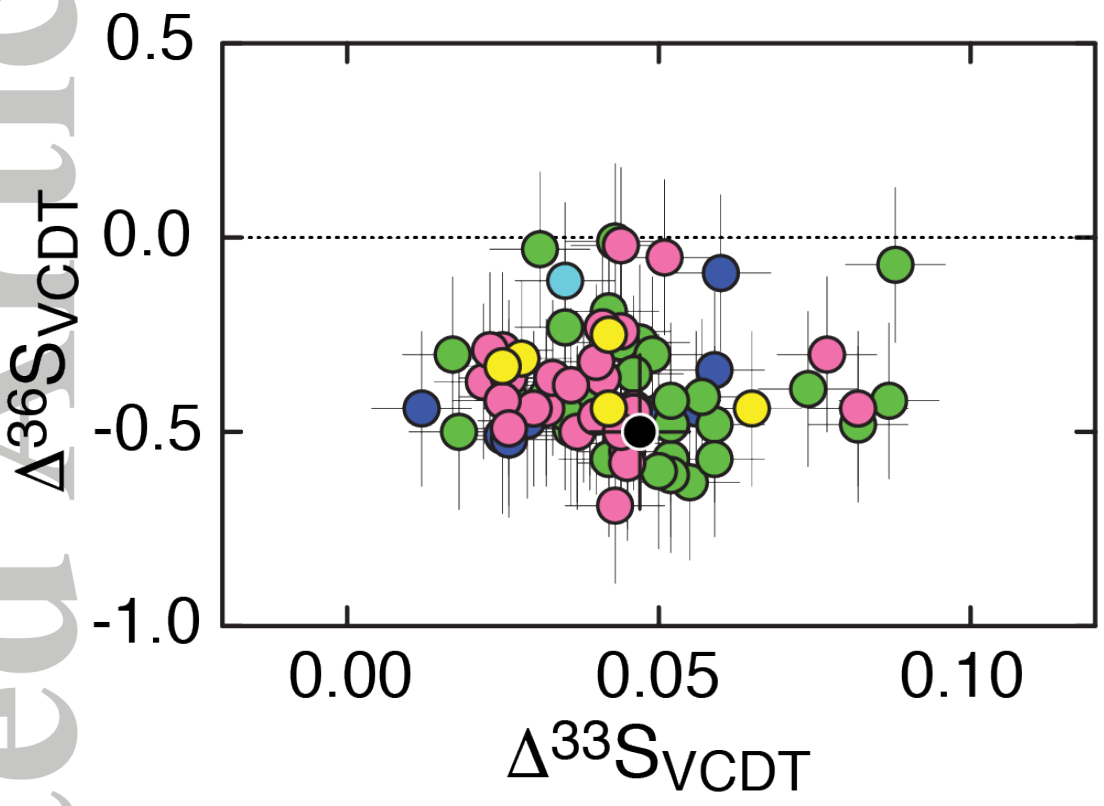

Figure 3. A box and whisker analysis of the different data populations. The errors reflect 95 % confidence intervals on the population, with median values plotted as the center bars.

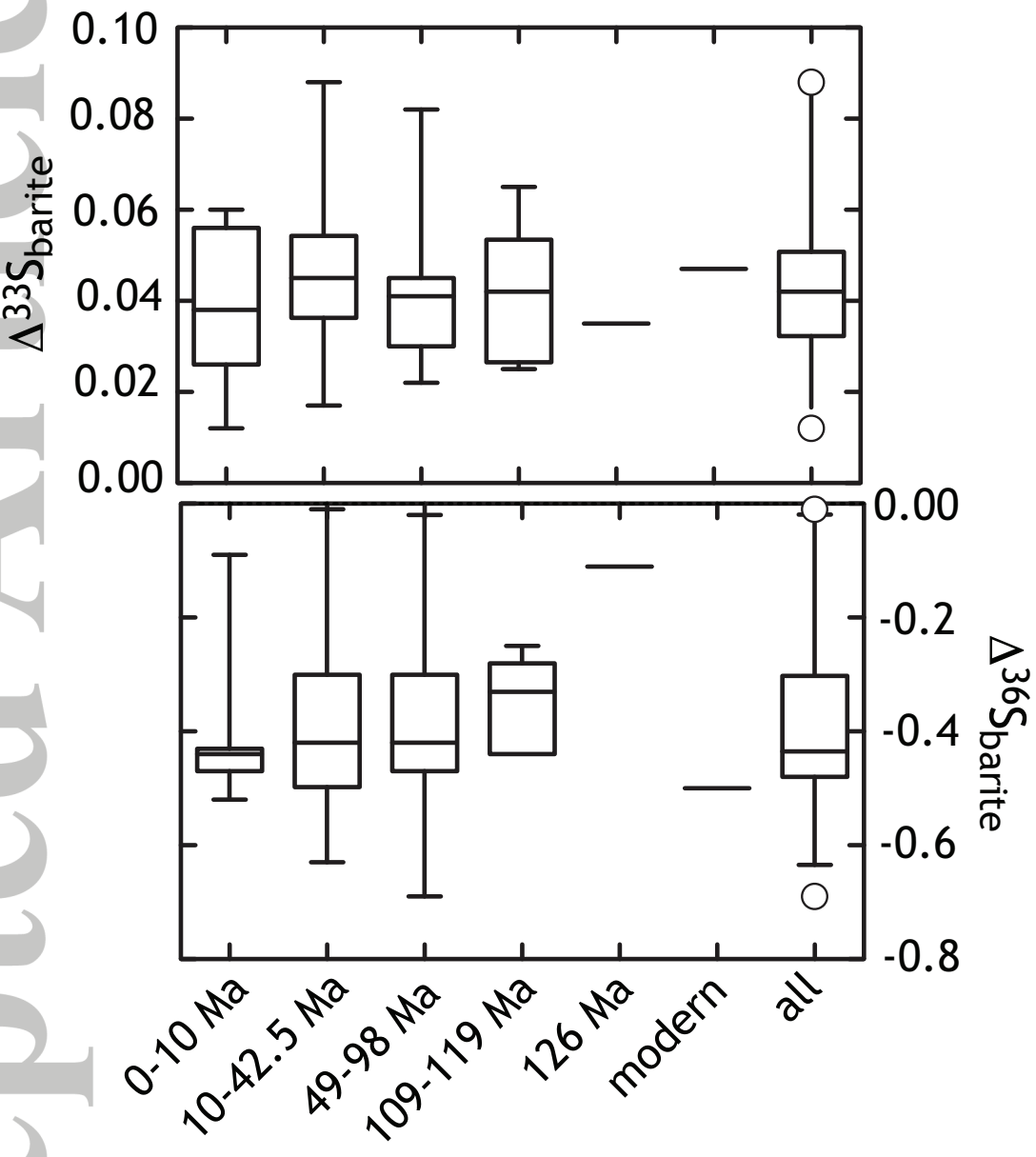

Figure 4. The barite record of $\Delta^{33}S$ (top) versus $\Delta^{36}S$ (bottom) versus time. The color coding is shared with Figure 1 and errors are 2 σ.

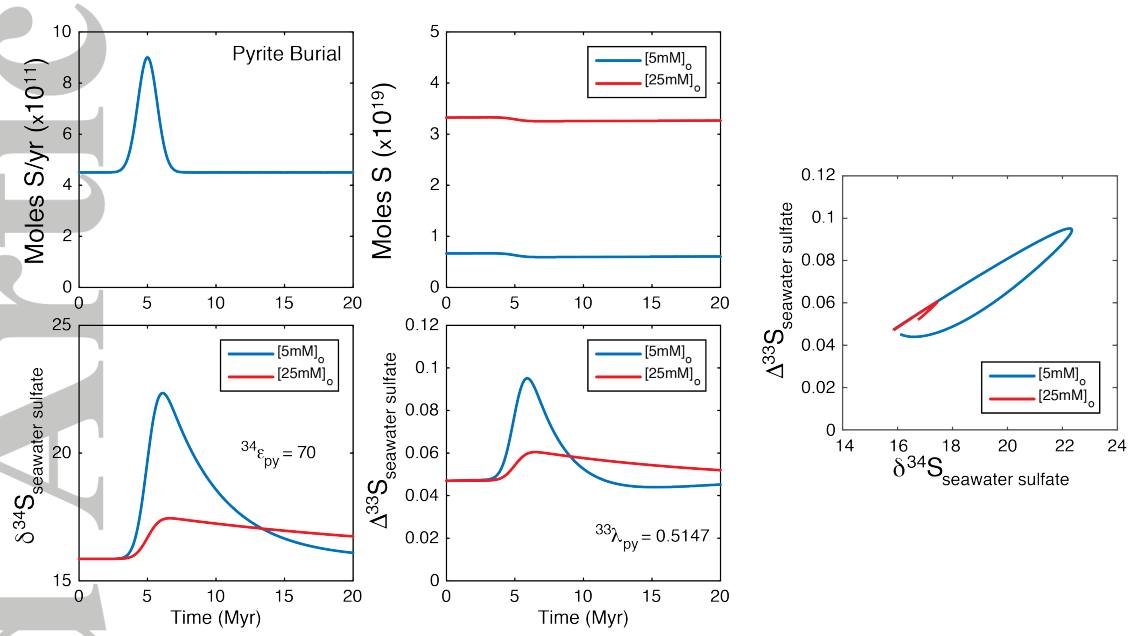

Figure 5. A simple one box sulfate model whereby the sensitivity of $\Delta^{33}S$ can be demonstrated, here as a function of changing pyrite burial over a 1 million year period. Moving from the upper left, we model the change in pyrite burial as it propagates through the mass of seawater sulfate (upper right), the $\delta^{34}S$ of sulfate (lower left) and the $\Delta^{33}S$ of sulfate (lower right). Fractionation factors were derived from [35@Masterson et al., ,10@Farquhar et al., 2003].

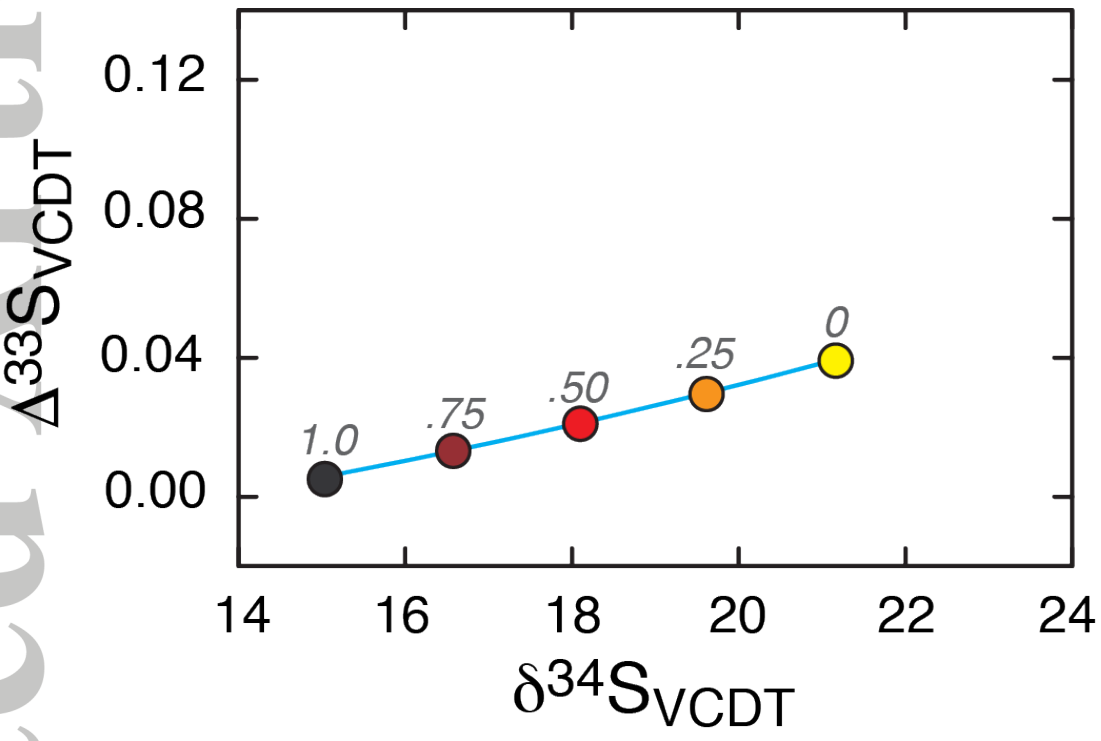

Figure 6. **A simple mixing relationship demonstrating the consequences of reintroducing evaporitic sulfate back into the ocean.**